Calculation of Three-Dimensional, Viscous Flow Through Turbomachinery Blade Passage by Parabolic Marching

Theodore Katsanis*
NASA Lewis Research Center, Cleveland, Ohio

The three-dimensional compressible Navier-Stokes equations are formulated in a rotating coordinate system, so as to include centrifugal and Coriolis forces. The equations are parabolized by using a previously calculated inviscid static pressure field. The thin-layer Navier-Stokes approximation, which neglects streamwise diffusion, is used. A body-fitted coordinate system is used. The streamwise momentum equation is uncoupled from the cross-stream momentum equation by using contravariant momentum components and then using the contravariant velocity components as primary unknowns. To reduce problems with small separated regions, the Reyhner and Flugge-Lotz approximation is used. The energy equation is included to allow for calculation of heat transfer. The flow may be laminar or a simple eddy-viscosity turbulence model may be used. A number of curved ducts and an axial stator have been analyzed, including cases for which experimental data are available.

Nomenclature

e = total internal energy
H = total enthalpy
I = rothalpy
J = transformation Jacobian from Cartesian to (ξ,η,ζ) coordinates
J_1 = transformation Jacobian from Cartesian to cylindrical coordinates
J_2 = transformation Jacobian from cylindrical to (ξ,η,ζ) coordinates
k = thermal conductivity
p = pressure
r = radius
t = time
V = absolute velocity
W = relative velocity
x,y,z = Cartesian coordinates
γ = specific heat ratio
ζ = hub-to-shroud grid coordinate
η = blade-to-blade grid coordinate
θ = angular coordinate, radians
μ = viscosity
ξ = streamwise grid coordinate
ρ = density
τ = stress
ω = angular velocity

Subscripts

r = r component
z = z component
θ = θ component

Superscripts

ζ = ζ contravariant component
η = η contravariant component
ξ = ξ contravariant component

Received April 30, 1985; presented as Paper 85-1405 at the AIAA/SAE/ASME 21st Joint Propulsion Conference, Monterey, CA, July 8-10, 1985; revision received Sept. 26, 1985. This paper is declared a work of the U.S. Government and therefore is in the public domain.

*Research Scientist. Associate Fellow AIAA.

Introduction

WELL-GUIDED internal flow without separated regions behaves in a parabolic manner[1] so that the flowfield can be predicted using a parabolic streamwise marching method. Several computer codes have been written for calculating three-dimensional viscous flow through ducts of fairly complex geometry.[2-4] Reference 2 contains an extensive survey of "parabolic" approximations, primarily for external flow. The same principles can be applied to calculate flow through the blades of the turbomachine. However, there are several distinguishing aspects of the flow through a turbomachine blade row: 1) the blade row may be rotating, 2) the hub and shroud are usually surfaces of revolution, 3) the passage has four walls meeting at an angle, 4) the flow may be periodic upstream and downstream of the blade, and 5) the shroud is usually stationary for a rotating blade row. The method and computer code described here is especially formulated to satisfy and take advantage of these particular aspects of the flow.

The parabolic marching calculation is analagous to calculation of a three-dimensional boundary layer. An inviscid pressure field is used as an initial pressure field; then a single-pass calculation through the length of the blade passage is made. To simplify the application of boundary conditions on complex blade surfaces, a body-fitted coordinate system is used. This body-fitted coordinate system has one coordinate that generates circles about the axis of rotation. One of the coordinate surfaces coincides with the hub of the blade row and another coincides with the shroud. This type of coordinate system eases implementation of periodic boundary conditions upstream and downstream of the blade row; on the other hand, this type of coordinate system cannot be orthogonal.

In the spirit of Patankar and Spalding,[1] the streamwise momentum calculation is uncoupled from the cross-stream momentum calculation. This uncoupling is accomplished by using contravariant components of the momentum equation and using contravariant velocity components as the primary unknowns.[5,6] The downstream contravariant velocity components are always calculated implicitly for stability. To calculate the streamwise contravariant velocity components at the new downstream station, it is assumed that the static pressure and cross-stream contravariant velocity components are known at the previous upstream station. The streamwise pressure gradient is varied by a constant amount over the passage cross section so that global mass flow through the entire passage is conserved. The cross-section contravariant velocity components are calculated at the next downstream station based on the inviscid pressure field and using the last calculated streamwise contravariant velocity components. Continuity is then checked for each mesh region and cross-stream pressure gradient is adjusted so that continuity is satisfied for every mesh region. Iteration is required at each station so that both cross-stream momentum and local continuity are satisfied. For turbulent flow, the Baldwin-Lomax eddy-viscosity turbulence model is used.[7]

Parabolic Marching through a Turbomachine Passage

Contravariant Form of the Navier-Stokes Equations for a Rotating Nonorthogonal Coordinate System

The continuity equation in conservation form in cylindrical coordinates is

$$\frac{\partial}{\partial t}(r\rho)+\frac{\partial}{\partial r}(r\rho W_r)+\frac{\partial}{\partial\theta}(\rho W_\theta)+\frac{\partial}{\partial z}(r\rho W_z)=0 \tag{1}$$

In cylindrical (r,θ,z) coordinates the Navier-Stokes equations may be written in weak conservation form as follows [Eq. (1.29) of Ref. 8]:

$$\frac{\partial}{\partial t}(r\rho V_r)+\frac{\partial}{\partial r}(r\rho V_r^2)+\frac{\partial}{\partial\theta}(\rho V_r V_\theta)+\frac{\partial}{\partial z}(r\rho V_r V_z)-\rho V_\theta^2$$
$$=\frac{\partial}{\partial r}(r\tau_{rr}-rp)+\frac{\partial}{\partial\theta}(\tau_{r\theta})+\frac{\partial}{\partial z}(r\tau_{rz})-\tau_{\theta\theta}+p$$

$$\frac{\partial}{\partial t}(r\rho V_\theta)+\frac{\partial}{\partial r}(r\rho V_r V_\theta)+\frac{\partial}{\partial\theta}(\rho V_\theta^2)+\frac{\partial}{\partial z}(r\rho V_\theta V_z)+\rho V_r V_\theta$$
$$=\frac{\partial}{\partial r}(r\tau_{r\theta})+\frac{\partial}{\partial\theta}(\tau_{\theta\theta}-p)+\frac{\partial}{\partial z}(r\tau_{\theta z})+\tau_{r\theta}$$

$$\frac{\partial}{\partial t}(r\rho V_z)+\frac{\partial}{\partial r}(r\rho V_r V_z)+\frac{\partial}{\partial\theta}(\rho V_\theta V_z)+\frac{\partial}{\partial z}(r\rho V_z^2)$$
$$=\frac{\partial}{\partial r}(r\tau_{rz})+\frac{\partial}{\partial\theta}(\tau_{r\theta})+\frac{\partial}{\partial z}(r\tau_{zz}-p)$$

The change to a rotating coordinate system is accomplished by the change of variables as follows:

$$t'=t \qquad W_r=V_r$$
$$r'=r \qquad W_\theta=V_\theta-\omega r$$
$$\theta'=\theta-\omega t \qquad W_z=V_z$$
$$z'=z$$

The partial derivatives with respect to t then become

$$\frac{\partial}{\partial t}=\frac{\partial}{\partial t'}-\omega\frac{\partial}{\partial\theta}$$

The resulting Navier-Stokes equations for rotating cylindrical coordinates are now (the prime has been dropped)

$$\frac{\partial}{\partial t}(r\rho W_r)+\frac{\partial}{\partial r}(r\rho W_r^2)+\frac{\partial}{\partial\theta}(\rho W_r W_\theta)+\frac{\partial}{\partial z}(r\rho W_r W_z)$$
$$=\rho V_\theta^2-r\frac{\partial p}{\partial r}-\tau_{\theta\theta}+\frac{\partial}{\partial r}(r\tau_{rr})+\frac{\partial}{\partial\theta}(\tau_{r\theta})+\frac{\partial}{\partial z}(r\tau_{rz}) \tag{2}$$

$$\frac{\partial}{\partial t}(r\rho W_\theta)+\frac{\partial}{\partial r}(r\rho W_\theta W_r)+\frac{\partial}{\partial\theta}(\rho W_\theta^2)+\frac{\partial}{\partial z}(r\rho W_\theta W_z)$$
$$=-\rho W_r(W_\theta+2\omega r)-\frac{\partial p}{\partial\theta}+\tau_{r\theta}+\frac{\partial}{\partial r}(r\tau_{r\theta})$$
$$+\frac{\partial}{\partial\theta}(\tau_{\theta\theta})+\frac{\partial}{\partial z}(r\tau_{r\theta}) \tag{3}$$

$$\frac{\partial}{\partial t}(r\rho W_z)+\frac{\partial}{\partial r}(r\rho W_z W_r)+\frac{\partial}{\partial\theta}(\rho W_z W_\theta)+\frac{\partial}{\partial z}(r\rho W_z^2)$$
$$=-r\frac{\partial p}{\partial z}+\frac{\partial}{\partial r}(r\tau_{rz})+\frac{\partial}{\partial\theta}(\tau_{\theta z})+\frac{\partial}{\partial z}(r\tau_{zz}) \tag{4}$$

Finally, the energy equation in conservation form is

$$\frac{\partial e}{\partial t}+\nabla\cdot\Big((e+p)\bar{V}\Big)=\nabla\cdot k\nabla T+V\cdot(\hat{\bar{\tau}}\bar{V})$$

This is expanded in cylindrical coordinates, and transformed to rotating coordinates using

$$\frac{\partial}{\partial t}=\frac{\partial}{\partial t'}-\omega\frac{\partial}{\partial\theta}$$

Also, rothalpy I is introduced, using the relation

$$e+p=\rho I+\omega r\rho V_\theta$$

The energy equation in conservation form for rotating cylindrical coordinates and in terms of rothalpy is

$$\frac{\partial}{\partial t}\Big[r(\rho I-p)\Big]+r\nabla\cdot(\rho I\bar{W})=r\nabla\cdot k\nabla T+r\nabla\cdot(\hat{\bar{\tau}}\bar{W})$$

or

$$\frac{\partial}{\partial t}r(\rho I-p)+\frac{\partial}{\partial r}(r\rho IW_r)+\frac{\partial}{\partial\theta}(\rho IW_\theta)+\frac{\partial}{\partial z}(r\rho IW_z)$$
$$=\frac{\partial}{\partial r}\left(rk\frac{\partial T}{\partial r}\right)+\frac{\partial}{\partial\theta}\left(\frac{k}{r}\frac{\partial T}{\partial\theta}\right)+\frac{\partial}{\partial z}\left(rk\frac{\partial T}{\partial z}\right)$$
$$+\frac{\partial}{\partial r}\Big[r(W_r\tau_{rr}+W_\theta\tau_{r\theta}+W_z\tau_{rz})\Big]$$
$$+\frac{\partial}{\partial\theta}(W_r\tau_{r\theta}+W_\theta\tau_{\theta\theta}+W_z\tau_{\theta z})$$
$$+\frac{\partial}{\partial z}\Big[r(W_r\tau_{rz}+W_\theta\tau_{\theta z}+W_z\tau_{zz})\Big] \tag{5}$$

Equations (1-5) can be written in compact form as

$$\partial_t q+\partial_r E+\partial_\theta F+\partial_z G=K+\partial_r R+\partial_\theta S+\partial_z T \tag{6}$$

where

$$q=r\begin{bmatrix}\rho\\ \rho W_r\\ \rho W_\theta\\ \rho W_z\\ \rho I-p\end{bmatrix},\quad E=r\begin{bmatrix}\rho W_r\\ \rho W_r^2\\ \rho W_r W_\theta\\ \rho W_r W_z\\ \rho W_r I\end{bmatrix},\quad F=\begin{bmatrix}\rho W_\theta\\ \rho W_\theta W_r\\ \rho W_\theta^2\\ \rho W_\theta W_z\\ \rho W_\theta I\end{bmatrix}$$

$$G=r\begin{bmatrix}\rho W_z\\ \rho W_z W_r\\ \rho W_z W_\theta\\ \rho W_z^2\\ \rho W_z I\end{bmatrix},\quad K=\begin{bmatrix}0\\ \rho V_\theta^2-\dfrac{r\partial p}{\partial r}-\tau_{\theta\theta}\\ \tau_{r\theta}-\dfrac{\partial p}{\partial\theta}-\rho W_r(W_\theta+2\omega r)\\ -r\dfrac{\partial p}{\partial z}\\ 0\end{bmatrix}$$

$$R=r\begin{bmatrix}0\\ \tau_{rr}\\ \tau_{r\theta}\\ \tau_{rz}\\ W_r\tau_{rr}+W_\theta\tau_{r\theta}+W_z\tau_{rz}+\dfrac{k\partial T}{\partial r}\end{bmatrix}$$

$$S=\begin{bmatrix}0\\ \tau_{r\theta}\\ \tau_{\theta\theta}\\ \tau_{\theta z}\\ W_r\tau_{r\theta}+W_\theta\tau_{\theta\theta}+W_z\tau_{\theta z}+k\dfrac{\partial T}{r\partial\theta}\end{bmatrix}$$

$$T=r\begin{bmatrix}0\\ \tau_{rz}\\ \tau_{\theta z}\\ \tau_{zz}\\ W_r\tau_{rz}+W_\theta\tau_{\theta z}+W_z\tau_{zz}+k\dfrac{\partial T}{\partial z}\end{bmatrix}$$

Equation (6) can be transformed to an arbitrary nonorthogonal rotating coordinate system (ξ,η,ζ) using the chain rule. When this is done, considerable simplification occurs by combining terms properly[9,10] and by using the contravariant velocity components as variables. Note that terms such as

$$\left(\frac{\xi_r}{J_2}\right)_\xi+\left(\frac{\eta_r}{J_2}\right)_\eta+\left(\frac{\zeta_r}{J_2}\right)_\zeta$$

are equal to zero,[11] so that factors like ξ_r/J_2 can be moved inside the derivative. The form of equations is now

$$\partial_t\hat{q}+\partial_\xi\hat{E}+\partial_\eta\hat{F}+\partial_\zeta\hat{G}=\hat{K}+\partial_\xi\hat{R}+\partial_\eta\hat{S}+\partial_\zeta\hat{T} \tag{7}$$

where

$$\hat{q}=J^{-1}\begin{bmatrix}\rho\\ \rho W_r\\ \rho W_r\\ \rho W_z\\ \rho I-p\end{bmatrix},\quad \hat{E}=J^{-1}\begin{bmatrix}\rho W^\xi\\ \rho W^\xi W_r\\ \rho W^\xi W_\theta\\ \rho W^\xi W_z\\ \rho W^\xi I\end{bmatrix}$$

$$\hat{F}=J^{-1}\begin{bmatrix}\rho W^\eta\\ \rho W^\eta W_r\\ \rho W^\eta W_\theta\\ \rho W^\eta W_z\\ \rho W^\eta I\end{bmatrix},\quad \hat{G}=J^{-1}\begin{bmatrix}\rho W^\zeta\\ \rho W^\zeta W_r\\ \rho W^\zeta W_\theta\\ \rho W^\zeta W_z\\ \rho W^\zeta I\end{bmatrix}$$

$$\hat{R}=J^{-1}\begin{bmatrix}0\\ \tau_r^\xi\\ \tau_\theta^\xi\\ \tau_z^\xi\\ \xi_r\beta_r+\dfrac{\xi_\theta\beta_\theta}{r}+\xi_z\beta_z\end{bmatrix},\quad \hat{S}=J^{-1}\begin{bmatrix}0\\ \tau_r^\eta\\ \tau_\theta^\eta\\ \tau_z^\eta\\ \eta_r\beta_r+\dfrac{\eta_\theta\beta_\theta}{r}+\eta_z\beta_z\end{bmatrix}$$

$$\hat{T}=J^{-1}\begin{bmatrix}0\\ \tau_r^\zeta\\ \tau_\theta^\zeta\\ \tau_z^\zeta\\ \zeta_r\beta_r+\dfrac{\zeta_\theta\beta_r}{r}+\zeta_z\beta_z\end{bmatrix}$$

$$\hat{K}=J^{-1}\begin{bmatrix}0\\ \dfrac{\rho V_\theta^2}{r}-\dfrac{\partial p}{\partial r}-\dfrac{\tau_{\theta\theta}}{r}\\ \dfrac{\tau_{r\theta}}{r}-\dfrac{\partial p}{r\partial\theta}-\rho W_r\dfrac{(W_\theta+2W_r)}{r}\\ -\dfrac{\partial p}{\partial z}\\ 0\end{bmatrix}$$

$$W^\xi=\xi_r W_r+\xi_\theta\left(\frac{W_\theta}{r}\right)+\xi_z W_z,\quad W^\eta=\eta_r W_r+\eta_\theta\left(\frac{W_\theta}{r}\right)+\eta_z W_z$$

$$W^\zeta=\zeta_r W_r+\zeta_\theta\left(\frac{W_\theta}{r}\right)+\zeta_z W_z,\quad \tau_r^\xi=\xi_r\tau_{rr}+\xi_\theta\left(\frac{\tau_{r\theta}}{\tau}\right)+\xi_z\tau_{rz}$$

$$\tau_\theta^\xi=\xi_r\tau_{r\theta}+\xi_\theta\left(\frac{\tau_{\theta\theta}}{r}\right)+\xi_z\tau_{\theta z},\quad \tau_z^\xi=\xi_r\tau_{rz}+\xi_\theta\left(\frac{\tau_{\theta z}}{r}\right)+\xi_z\tau_{zz}$$

$$\tau_r^\eta=\eta_r\tau_{rr}+\eta_\theta\left(\frac{\tau_{\theta r}}{r}\right)+\eta_z\tau_{rz},\quad \tau_\theta^\eta=\eta_r\tau_{r\theta}+\eta_\theta\left(\frac{\tau_{\theta\theta}}{r}\right)+\eta_z\tau_{\theta z}$$

$$\tau_z^\eta=\eta_r\tau_{rz}+\eta_\theta\left(\frac{\tau_{\theta z}}{r}\right)+\eta_z\tau_{zz},\quad \tau_r^\zeta=\zeta_r\tau_{rr}+\zeta_\theta\left(\frac{\tau_{r\theta}}{r}\right)+\zeta_z\tau_{rz}$$

$$\tau_\theta^\zeta=\zeta_r\tau_{r\theta}+\zeta_\theta\left(\frac{\tau_{\theta\theta}}{r}\right)+\zeta_z\tau_{\theta z},\quad \tau_z^\zeta=\zeta_r\tau_{rz}+\zeta_\theta\left(\frac{\tau_{\theta z}}{r}\right)+\zeta_z\tau_{zz}$$

$$\beta_r=W_r\tau_{rr}+W_\theta\tau_{r\theta}+W_z\tau_{rz}+k\partial_r T$$

$$\beta_\theta=W_r\tau_{r\theta}+W_\theta\tau_{\theta\theta}+W_z\tau_{\theta z}+k\frac{\partial_\theta T}{r}$$

$$\beta_z=W_r\tau_{rz}+W_\theta\tau_{\theta z}+W_z\tau_{zz}+k\partial_z T$$

Equation (7) still has cylindrical momentum components. It is desired to utilize momentum components aligned with the mesh, so that the streamwise momentum is easily uncoupled from the cross-stream momentum components. This is accomplished by taking the contravariant velocity components. For example, the contravariant ξ momentum component is ξ_r(r momentum) plus η_θ/r(θ momentum) plus ζ_z(z momentum). This results in

$$\partial_t\hat{q}+\partial_\xi\hat{\hat{E}}+\partial_\eta\hat{\hat{F}}+\partial_\zeta\hat{\hat{G}}=\partial_\xi\hat{\hat{R}}+\partial_\eta\hat{\hat{S}}+\partial_\zeta\hat{\hat{T}}+\hat{\hat{K}} \tag{8}$$

where

$$\hat{q}=\frac{1}{J}\begin{bmatrix}\rho\\ \rho W^\xi\\ \rho W^\eta\\ \rho W^\zeta\\ \rho I-p\end{bmatrix},\quad \hat{\hat{E}}=\frac{1}{J}\begin{bmatrix}\rho W^\xi\\ \rho W^\xi W^\xi\\ \rho W^\xi W^\eta\\ \rho W^\xi W^\zeta\\ \rho W^\xi I\end{bmatrix},\quad \hat{\hat{F}}=\frac{1}{J}\begin{bmatrix}\rho W^\eta\\ \rho W^\eta W^\xi\\ \rho W^\eta W^\eta\\ \rho W^\eta W^\zeta\\ \rho W^\eta I\end{bmatrix}$$

$$\hat{\hat{G}}=\frac{1}{J}\begin{bmatrix}\rho W^\zeta\\ \rho W^\zeta W^\xi\\ \rho W^\zeta W^\eta\\ \rho W^\zeta W^\zeta\\ \rho W^\zeta I\end{bmatrix},\quad \hat{\hat{R}}=\frac{1}{J}\begin{bmatrix}0\\ \xi_r\tau_r^\xi+\dfrac{\xi_\theta\tau_\theta^\xi}{r}+\xi_z\tau_z^\xi\\ \eta_r\tau_r^\xi+\dfrac{\eta_\theta\tau_\theta^\xi}{r}+\eta_z\tau_z^\xi\\ \zeta_r\tau_r^\xi+\dfrac{\zeta_\theta\tau_\theta^\xi}{r}+\zeta_z\tau_z^\xi\\ \xi_r\beta_r+\dfrac{\xi_\theta\beta_\theta}{r}+\xi_z\beta_z\end{bmatrix}$$

$$\hat{\hat{S}}=\frac{1}{J}\begin{bmatrix}0\\ \xi_r\tau_r^\eta+\dfrac{\xi_\theta\tau_\theta^\eta}{r}+\xi_z\tau_z^\eta\\ \eta_r\tau_r^\eta+\dfrac{\eta_\theta\tau_\theta^\eta}{r}+\eta_z\tau_z^\eta\\ \zeta_r\tau_r^\eta+\dfrac{\zeta_\theta\tau_\theta^\eta}{r}+\zeta_z\tau_z^\eta\\ \eta_r\beta_r+\dfrac{\eta_\theta\beta_\theta}{r}+\eta_z\beta_z\end{bmatrix}\qquad \hat{\hat{T}}=\frac{1}{J}\begin{bmatrix}0\\ \xi_r\tau_r^\zeta+\dfrac{\xi_\theta\tau_\theta^\zeta}{r}+\xi_z\tau_z^\zeta\\ \eta_r\tau_r^\zeta+\dfrac{\eta_\theta\tau_\theta^\zeta}{r}+\eta_z\tau_z^\zeta\\ \zeta_r\tau_r^\zeta+\dfrac{\zeta_\theta\tau_\theta^\zeta}{r}+\zeta_z\tau_r^\zeta\\ \zeta_r\beta_r+\dfrac{\zeta_\theta\beta_\theta}{r}+\zeta_z\beta_z\end{bmatrix}$$

$$\hat{\hat{K}}=\frac{1}{J}\begin{bmatrix}0\\ \rho G_{\xi\rho}-g^{\xi\xi}p_\xi-g^{\xi\eta}p_\eta-g^{\xi\zeta}p_\zeta-\dfrac{\xi_r\tau_{\theta\theta}}{r}+\dfrac{\xi_\theta\tau_{r\theta}}{r^2}\\ \rho G_{\eta\rho}-g^{\eta\xi}p_\xi-g^{\eta\eta}p_\eta-g^{\eta\zeta}p_\zeta-\dfrac{\eta_r\tau_{\theta\theta}}{r}+\dfrac{\eta_\theta\tau_{r\theta}}{r^2}\\ \rho G_{\zeta\rho}-g^{\zeta\xi}p_\xi-g^{\zeta\eta}p_\eta-g^{\zeta\zeta}p_\zeta-\dfrac{\zeta_r\tau_{\theta\theta}}{r}+\dfrac{\zeta_\theta\tau_{r\theta}}{r^2}\\ 0\end{bmatrix}$$

$$\begin{aligned}G_{\xi\rho}={}&W^\xi\left[(\xi_r)_\xi W_r+\left(\frac{\xi_\theta}{r}\right)_\xi W_\theta+(\xi_z)_\xi W_z\right]\\&+W^\eta\left[(\xi_r)_\eta W_r+\left(\frac{\xi_\theta}{r}\right)_\eta W_\theta+(\xi_z)_\eta W_z\right]\\&+W^\zeta\left[(\xi_r)_\zeta W_r+\left(\frac{\xi_\theta}{r}\right)_\zeta W_\theta+(\xi_z)_\zeta W_z\right]\\&+\frac{\xi_r V_\theta^2}{r}-\frac{\xi_\theta}{r^2}W_r(W_\theta+2\omega r)\end{aligned}$$

$$\begin{aligned}G_{\eta\rho}={}&W^\xi\left[(\eta_r)_\xi W_r+\left(\frac{\eta_\theta}{r}\right)_\xi W_\theta+(\xi_z)_\xi W_z\right]\\&+W^\eta\left[(\eta_r)_\eta W_r+\left(\frac{\eta_\theta}{r}\right)_\eta W_\theta+(\xi_z)_\eta W_z\right]\\&+W^\zeta\left[(\eta_r)_\zeta W_r+\left(\frac{\eta_\theta}{r}\right)_\zeta W_\theta+(\xi_z)_\zeta W_z\right]\\&+\frac{\eta_r V_\theta^2}{r}-\frac{\eta_\theta}{r^2}W_r(W_\theta+2\omega r)\end{aligned}$$

$$\begin{aligned}G_{\zeta\rho}={}&W^\zeta\left[(\zeta_r)_\xi W_r+\left(\frac{\zeta_\theta}{r}\right)_\xi W_\theta+(\zeta_z)_\xi W_z\right]\\&+W^\eta\left[(\zeta_r)_\eta W_r+\left(\frac{\zeta_\theta}{r}\right)_\eta W_\theta+(\zeta_z)_\eta W_z\right]\\&+W^\zeta\left[(\zeta_r)_\zeta W_r+\left(\frac{\zeta_\theta}{r}\right)_\zeta W_\theta+(\zeta_z)_\zeta W_z\right]\\&+\frac{\zeta_r V_\theta^2}{r}-\frac{\zeta_\theta}{r^2}W_r(W_\theta+2\omega r)\end{aligned}$$

The terms $g^{\xi\xi}$, $g^{\xi\eta}$, etc., are the elements of the contravariant metric tensor.

Derivation of the Navier-Stokes Equations for Parabolic Marching Through a Turbomachinery Blade Row

Equation (8) retains all of the terms from the original Navier-Stokes, continuity, and energy equations for a general nonorthogonal rotating coordinate system. Some terms will now be eliminated or neglected. Only steady relative flow is considered, so the time derivatives will be eliminated. Also, the thin-layer assumption is made so that all streamwise derivatives of viscous terms will be neglected. Further, the mesh used is not completely general, so that certain coordinate derivatives will be eliminated.

The coordinate system used is shown in Fig. 1. The ξ coordinate is in the streamwise direction, η the blade-to-blade direction, and ζ from hub to shroud. Since the hub and shroud are both usually surfaces of revolution, and to make it easier to apply periodic boundary conditions, the η coordinate lines will be circular arcs coincident with the θ coordinate lines. Hence, ξ and ζ are functions of r and z only and are independent of θ,

$$\xi=\xi(r,z),\qquad \xi_\theta=0$$

$$\eta=\eta(r,\theta,z)$$

$$\zeta=\zeta(r,z),\qquad \zeta_\theta=0$$

The required coordinate derivatives ξ_r, ξ_z, η_r, etc., are calculated from the coordinate derivatives of the inverse transformation, r_ξ, θ_ξ, etc., by the equations

$$\xi_z=\frac{-r_\zeta}{(r_\xi z_\zeta-r_\zeta z_\xi)},\quad \eta_z=\frac{(r_\zeta\theta_\xi-r_\xi\theta_\zeta)}{\theta_\eta(r_\xi z_\zeta-r_\zeta z_\xi)}$$

$$\zeta_z=\frac{r_\xi}{(r_\xi z_\zeta-r_\zeta z_\xi)},\quad \xi_\theta=0,\quad \eta_\theta=1/\theta_\eta,\quad \zeta_\theta=0$$

$$\xi_r=\frac{z_\zeta}{(r_\xi z_\zeta-r_\zeta z_\xi)},\quad \eta_r=\frac{(\theta_\zeta z_\xi-\theta_\xi z_\zeta)}{\theta_\eta(r_\xi z_\zeta-r_\zeta z_\xi)}$$

$$\zeta_r=\frac{-z_\xi}{(r_\xi z_\zeta-r_\zeta z_\xi)} \tag{9}$$

The Jacobian J is given by

$$J = \frac{-1}{r\theta_\eta (r_\xi z_\zeta - r_\zeta z_\xi)} \tag{10}$$

Since ξ is the streamwise direction, all ξ derivatives of the viscous terms are neglected. Further, by using the continuity equation, for any function φ, we have

$$\partial_\xi \rho\left(\frac{W^\xi}{J}\varphi\right) + \partial_\eta\left(\rho\frac{W^\eta}{J}\varphi\right) + \partial_\zeta\left(\rho\frac{W^\zeta}{J}\varphi\right)$$

$$= \rho\frac{W^\xi}{J}\varphi_\xi + \rho\frac{W^\eta}{J}\varphi_\eta + \rho\frac{W^\zeta}{J}\varphi_\zeta \tag{11}$$

Excluding continuity, the equations become

$$\rho\frac{W^\xi}{J}\partial_\xi H + \rho\frac{W^\eta}{J}\partial_\eta H + \rho\frac{W^\zeta}{J}\partial_\zeta H = \partial_\eta\tilde{S} + \partial_\zeta\tilde{T} + \tilde{K} \tag{12}$$

where

$$H = \begin{bmatrix} W_\xi \\ W^\eta \\ W^\zeta \\ I \end{bmatrix}, \quad \tilde{S} = J^{-1}\begin{bmatrix} \xi_r\tau_r^\eta + \xi_z\tau_z^\eta \\ \eta_r\tau_r^\eta + \eta_\theta\tau_\theta^\eta/r + \eta_z\tau_z^\eta \\ \zeta_r\tau_r^\eta + \zeta_z\tau_z^\eta \\ \eta_r\beta_r + \eta_\theta\beta_\theta/r + \eta_z\beta_z \end{bmatrix}$$

$$\tilde{T} = J^{-1}\begin{bmatrix} \xi_r\tau_r^\zeta + \xi_z\tau_z^\zeta \\ \eta_r\tau_r^\zeta + \eta_\theta\tau_\theta^\zeta/r + \eta_z\tau_z^\zeta \\ \zeta_r\tau_r^\zeta + \zeta_z\tau_z^\zeta \\ \zeta_r\beta_r + \zeta_z\beta_z \end{bmatrix}$$

$$\tilde{K} = J^{-1}\begin{bmatrix} \rho G_{\xi\rho} - g^{\xi\xi}p_\xi - g^{\xi\eta}p_\eta - g^{\xi\zeta}p_\zeta \\ \rho G_{\eta\rho} - g^{\eta\xi}p_\xi - g^{\eta\eta}p_\eta - g^{\eta\zeta}p_\zeta \\ \rho G_{\zeta\rho} - g^{\zeta\xi}p_\xi - g^{\zeta\eta}p_\eta - g^{\zeta\zeta}p_\zeta \\ 0 \end{bmatrix}$$

Consistent with the thin-boundary-layer assumption, order-of-magnitude arguments are used to simplify calculation of the stress tensor in terms of the contravariant velocity components. Terms that are important involve the second derivative of a velocity component parallel to a wall with respect to the distance from the same wall, whereas the derivative of a velocity component normal to a wall with respect to the same wall is negligible. Also, coordinate derivatives (ξ_r, η_r, etc.) are considered to vary slowly compared to the velocity components thermselves. Even with these simplifications, the calculation of the stress tensor is rather complicated and messy for the nonorthogonal grid used.

Numerical Solution Procedure

A FORTRAN program called PARAMAR has been written to solve Eq. (12) by parabolic marching. Equation (12) is the thin-layer Navier-Stokes equation for a rotating, body-fitted coordinate system. The ξ, η, and ζ coordinates are in the streamwise direction, blade-to-blade, and hub-to-shroud, respectively, as indicated in Fig. 1. The equations are parabolized by using a previously calculated inviscid static pressure field and neglecting streamwise diffusion terms. The pressure field may be obtained by the MERIDL and TSONIC codes[12,13] or from the Denton code.[14]

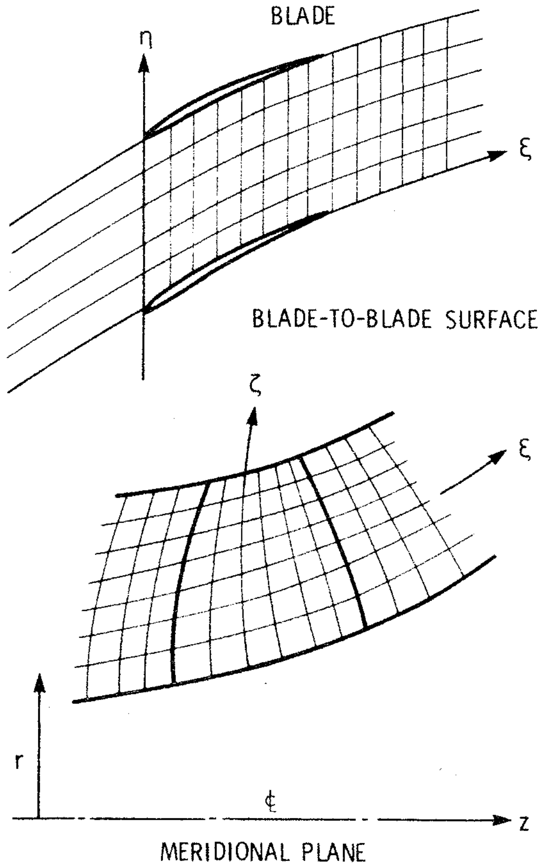

Fig. 1 Mesh and coordinate system.

The form of the three momentum equations and the energy equation is

$$\rho\frac{W^\xi}{J}\frac{\partial\varphi}{\partial\xi} + \rho\frac{W^\eta}{J}\frac{\partial\varphi}{\partial\eta} + \rho\frac{W^\zeta}{J}\frac{\partial\varphi}{\partial\zeta}$$

$$-\frac{\partial}{\partial\eta}a\frac{\partial\varphi}{\partial\eta} - \frac{\partial}{\partial\zeta}\left(b\frac{\partial\varphi}{\partial\zeta}\right) = S$$

where φ may be any contravariant velocity component or rothalpy. S is the remaining terms of the equation. The coefficients a and b and the source term S are different for each equation. By using a finite-difference approximation for the ξ derivative, the equation may be approximated as

$$\rho\frac{W^\xi}{J}(\varphi_{i+1} - \varphi_i) + \rho\frac{W^\eta}{J}\left(\frac{\partial\varphi}{\partial\eta}\right)_{i+1} + \rho\frac{W^\zeta}{J}\left(\frac{\partial\varphi}{\partial\zeta}\right)_{i+1}$$

$$-\left[\frac{\partial}{\partial\eta}\left(a\frac{\partial\varphi}{\partial\eta}\right)\right]_{i+1} - \left[\frac{\partial}{\partial\zeta}\left(b\frac{\partial\varphi}{\partial\zeta}\right)\right]_{i+1} = S_i$$

It is assumed that the mesh lines are coordinate lines and that $\xi_{i+1} - \xi_i = 1$. Similarly, for the other coordinates, it will be assumed that $\Delta\eta = \Delta\zeta = 1$. This equation is an implicit equation for φ_{i+1}. In finite difference form, the equation may be solved for φ_{i+1} directly by using the block tridiagonal algorithm (Ref. 15, p. 196).

Because of the importance of accurately calculating continuity for internal flow, a staggered mesh is used, much as suggested by Patankar and Spalding.[1] The mesh arrangement and numbering scheme is shown in Fig. 2. The three symbols show where each of the three contravariant components are located. The boomerang shape indicates the locations that have the same (integer) FORTRAN subscripts. In the (ξ,η,ζ) coordinates, the distance between like symbols is always one. The control volume for the continuity equation has a contravariant velocity at the center of each (transformed) face. Ths results in a very simple and accurate calculation of both local and global continuity. The finite difference equation for continuity for a control volume centered at $(\xi_{i+\frac{1}{2}},\eta_j,\zeta_k)$ is

$$\left(\rho\frac{W^\xi}{J}\right)_{i+i,j,k}-\left(\rho\frac{W^\xi}{J}\right)_{i,j,k}+\left(\rho\frac{W^\eta}{J}\right)_{i+\frac{1}{2},j+\frac{1}{2},k}$$
$$-\left(\rho\frac{W^\eta}{J}\right)_{i+\frac{1}{2},j-\frac{1}{2},k}+\left(\rho\frac{W^\zeta}{J}\right)_{i+\frac{1}{2},j,k+\frac{1}{2}}$$
$$-\left(\rho\frac{W^\zeta}{J}\right)_{i+\frac{1}{2},j,k-\frac{1}{2}}=0$$

and total mass flow for the passage is

$$\sum_{j=1}^{N}\sum_{k=1}^{M}\left(\rho\frac{W^\xi}{J}\right)_{i,j,k}$$

The importance of accurate calculation of global mass flow for internal passages cannot be overemphasized.

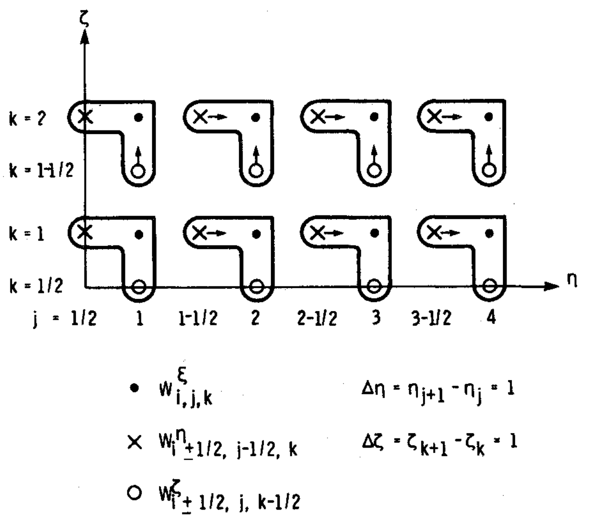

Fig. 2 Cross-section ($\eta\sqrt{\zeta}$) surface (mesh arrangement and numbering scheme for staggered grid).

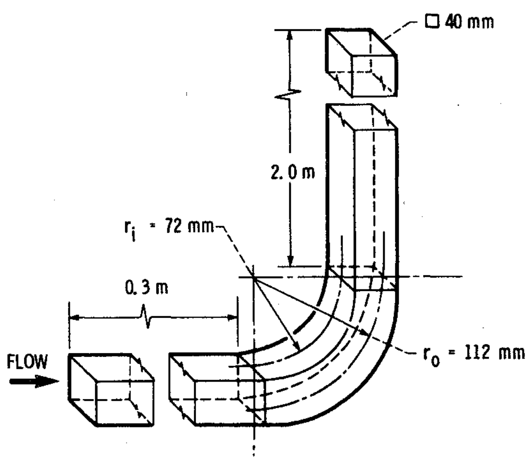

Fig. 3 Dimensions of curved duct.

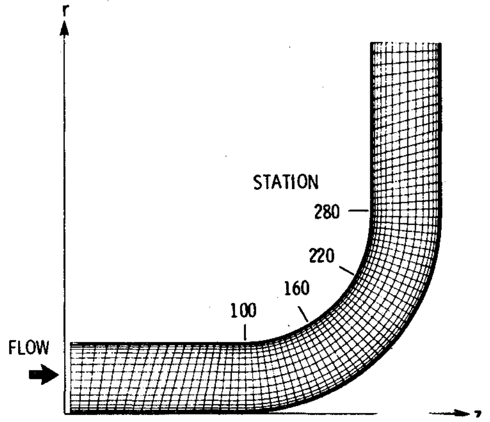

Fig. 4 Computational mesh for curved duct. Every fifth marching station shown. Every other streamwise mesh line shown.

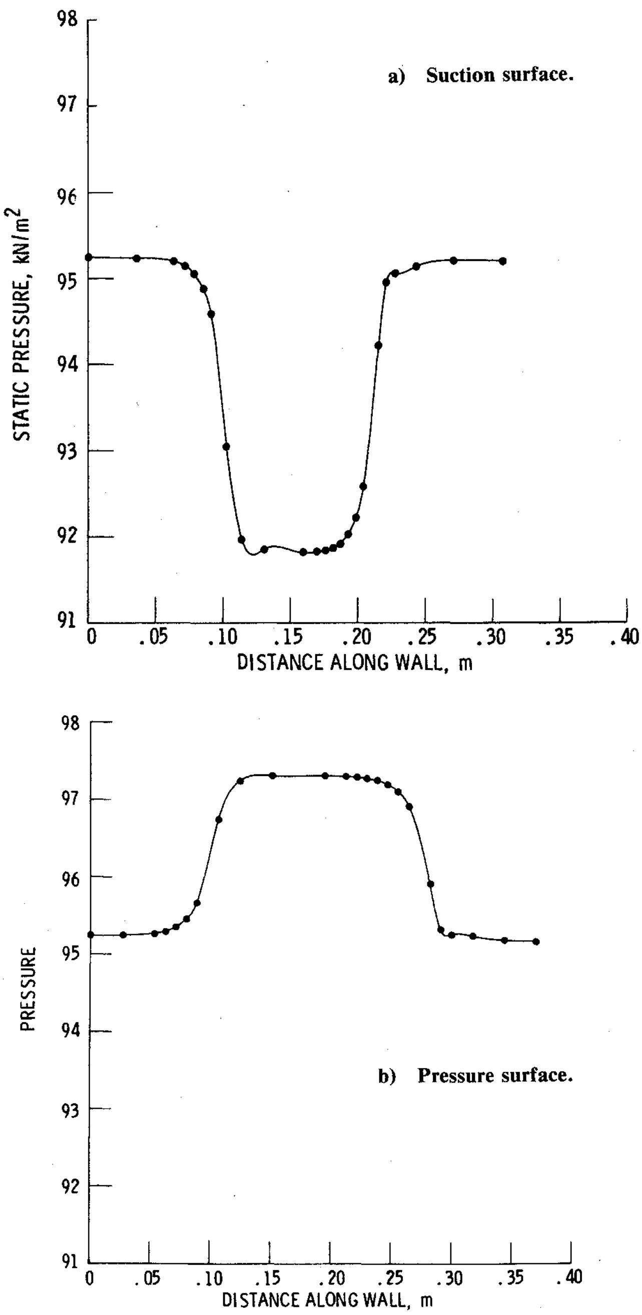

Fig. 5 Inviscid pressure for curved duct.

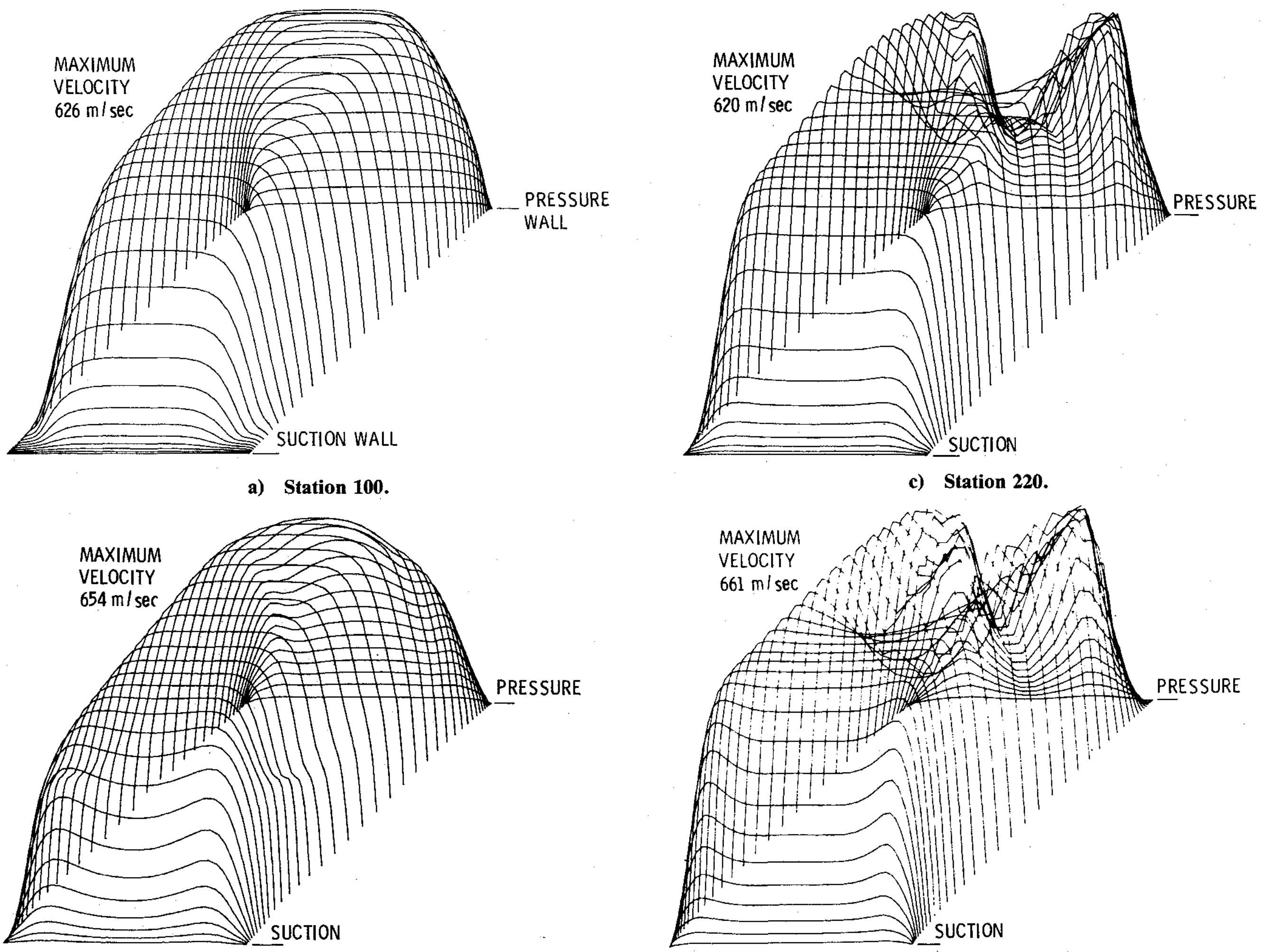

a) **Station 100.**

b) **Station 160.**

c) **Station 220.**

d) **Station 280.**

Fig. 6 Streamwise velocities for curved duct (see Fig. 4).

The streamwise (ξ) momentum equation is used to calculate the streamwise contravariant velocity components at the next streamwise station, using zero velocity boundary conditions. After calculating the downstream W^ξ, the mass flow at the downstream station will be low due to an increasing displacement thickness of the boundary layer. Hence, the pressure must be reduced at the downstream station, so that global continuity is satisfied. This is done by reducing the streamwise pressure gradient uniformly over the entire passage cross section.

The cross-stream momentum equations are used to calculate the cross-stream contravariant velocity components at the next station. Zero velocity boundary conditions are used. After calculating the cross-stream velocities, continuity is checked for each mesh region. In general, there will not be conservation of mass for each mesh region. An equation can be derived to calculate a correction to the pressure gradient needed in the two cross-stream momentum equations to give cross-stream velocity components that will satisfy continuity for each mesh region. The resulting equation resembles a finite difference Poisson equation for pressure over the downstream cross section. The derivation of this equation is explained very well in Ref. 1. This correction to the pressure gradient is needed to develop the correct cross flow within the boundary layer. Iteration is required at each station to satisfy both the continuity equation and the momentum equations.

If heat transfer is neglible, constant rothalpy may be assumed. The energy equation is used when heat transfer by convection and conduction is of interest. Then the rothalpy at the downstream station is calculated implicitly. Boundary conditions may specify adiabatic walls, specified wall temperature, or specified heat flux through the walls.

Cases of practical interest will have a turbulent boundary layer, of course. For this purpose, the Baldwin-Lomax eddy-viscosity model is used.[7] Provision is made for specifying a constant turbulent Prandtl number for the energy equation.

Numerical Examples

Several combinations of geometry, mesh, and flow conditions have been calculated for verifying the PARAMAR code. Most of this has been done for laminar flow to avoid the possibility of inaccuracy due to the turbulence model. Most of the geometry has been for straight ducts of various cross sections, at varying angles, and for accelerating and decelerating flow. In addition some curved ducts and turbomachine blades have been run, which are given as examples below.

Laminar Flow in a Curved Duct

The duct is shown in Fig. 3. Laser velocimeter measurements have been made by Taylor et al.[16] The measurements and calculations were made at a Reynolds number of 790, based on the hydraulic diameter of the duct. The calculation was started at 0.1 m upstream of the start of the bend with uniform flow. The mesh used for the calculation by PARAMAR is shown in Fig. 4. The inviscid pressure field

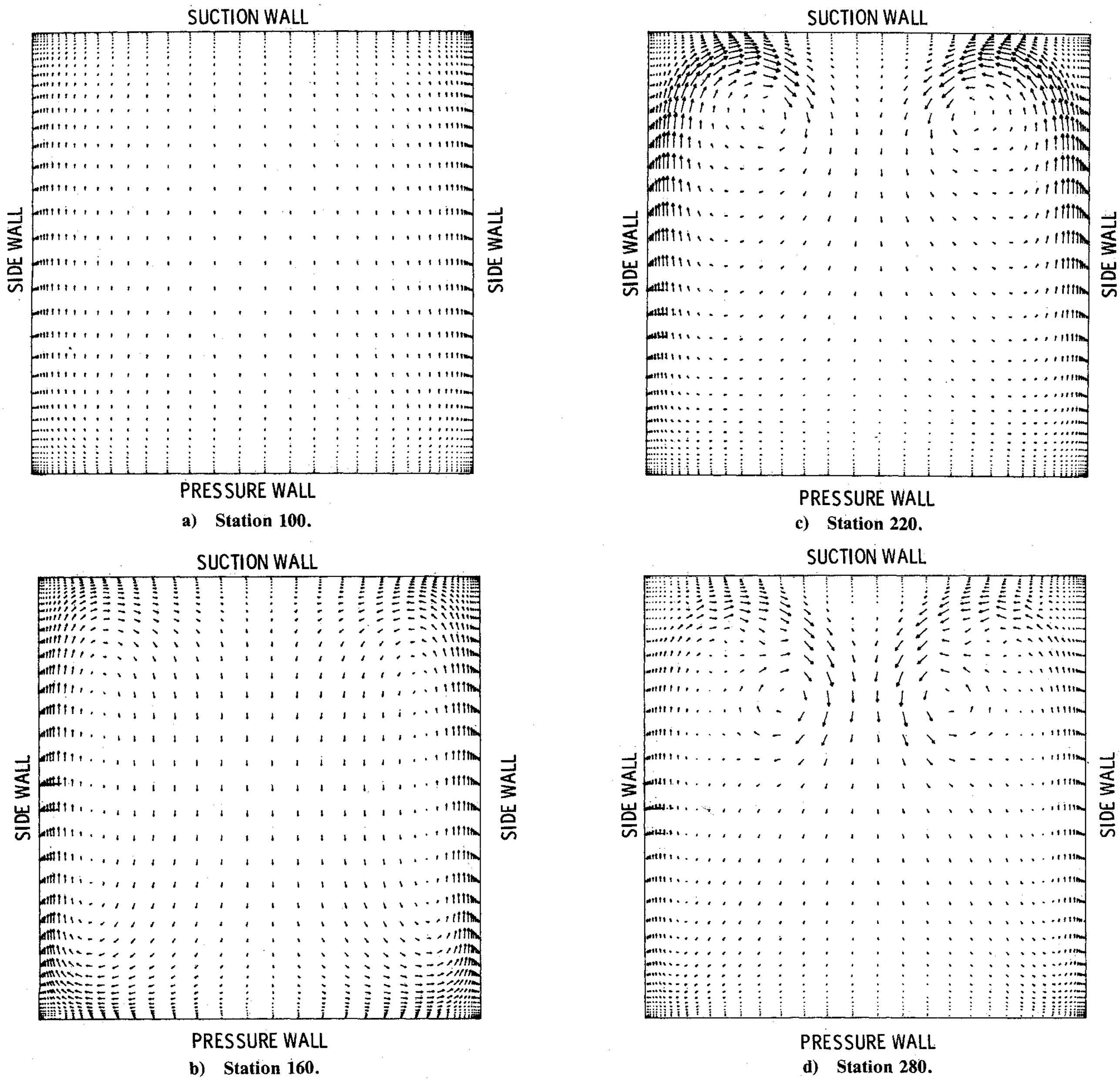

Fig. 7 Secondary velocity vectors for curved duct (see Fig. 4).

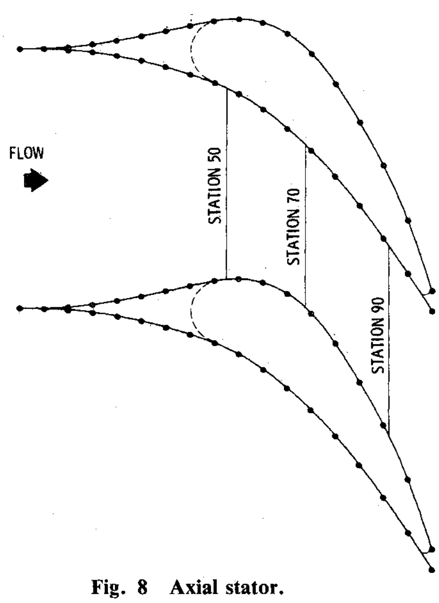

Fig. 8 Axial stator.

shown in Fig. 5 was obtained by using the Denton code.[14] Some difficulty was had with negative velocities on the pressure surface near the start of the bend. There is a strong adverse pressure gradient in this region, as shown in Fig. 5, which resulted in negative streamwise velocities being calculated. These negative velocities are closer to the wall than the experimental measurements shown in Ref. 16. When the streamwise velocities become negative, the streamwise momentum is increased to a small vlaue (2% of the freestream value for this case). Thus a small amount of momentum is being artificially added to the boundary layer. The added energy is negligible, but allows calculation through the small reverse flow region. This is a commonly used variation on the Reyhner and Flugge-Lotz approximation.[17]

Carpet plots of streamwise velocities and cross-section vector plots are shown in Figs. 6 and 7. The results agree qualitatively with the experimental results. In order to make a detailed comparison with the experiment, it is necessary to impose the proper flowfield at the start of the bend, which has not yet been done.

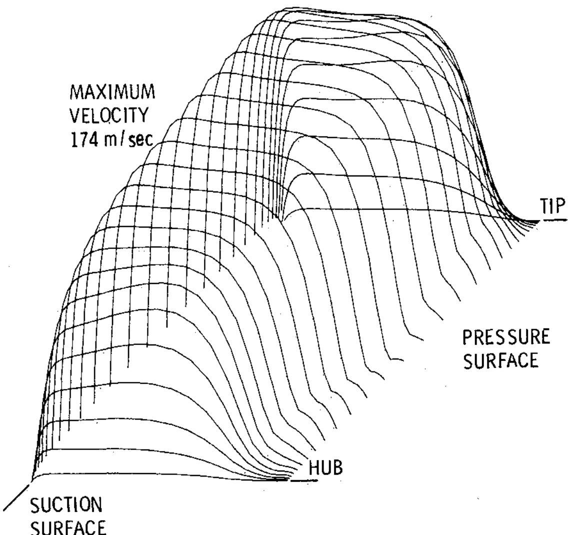

a) **Station 50.**

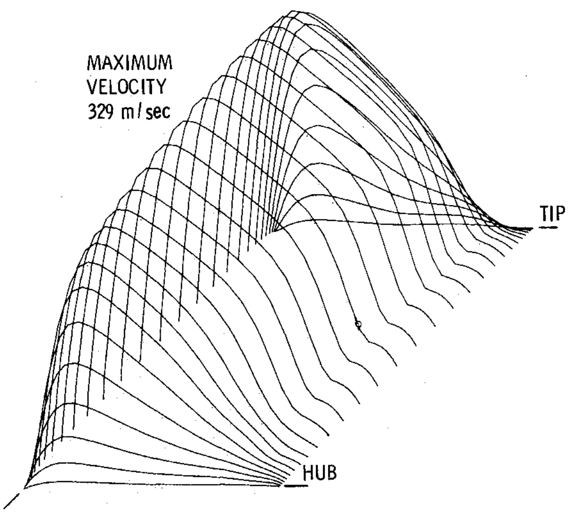

b) **Station 70.**

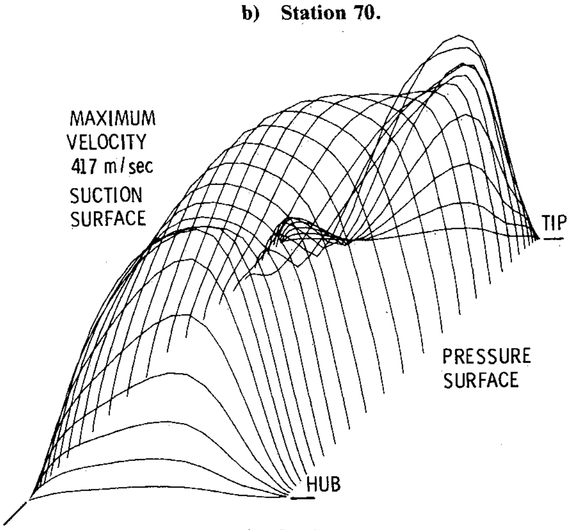

c) **Station 90.**

Fig. 9 Velocity magnitudes for axial stator (see Fig. 8).

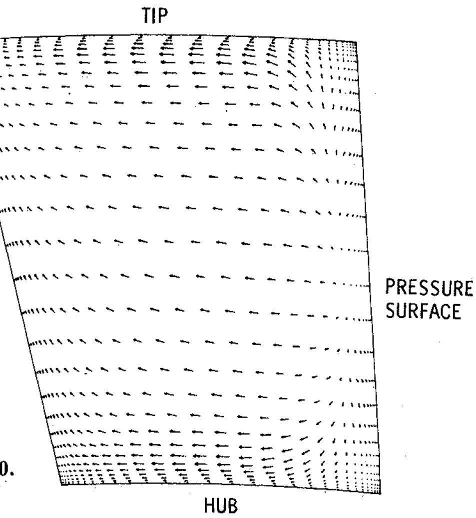

a) **Station 50.**

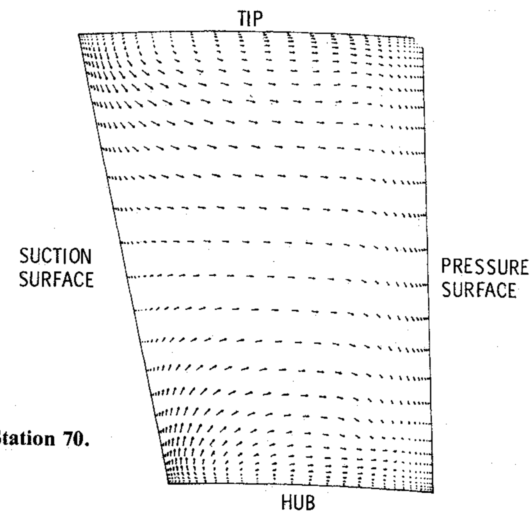

b) **Station 70.**

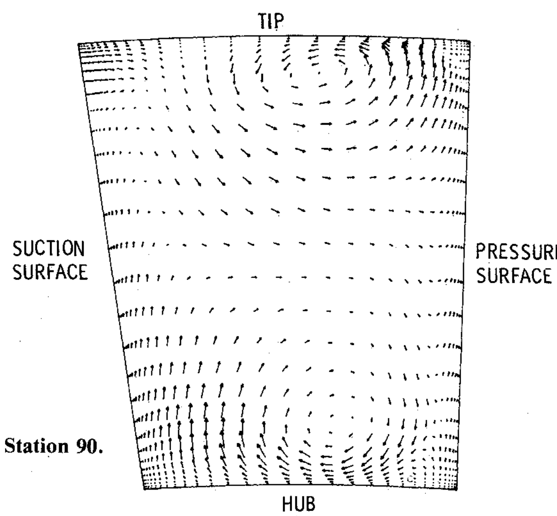

c) **Station 90.**

Fig. 10 Secondary velocity vectors for axial stator (see Fig. 8).

Flow Through an Axial Stator

The blade passage is shown in Fig. 8. A cusp has been added to the very blunt leading edge. Flow for this geometry has been calculated for laminar flow at a Reynolds number of 197, based on the upstream hydraulic diameter. An inviscid pressure field was obtained by the MERIDL and TSONIC codes.[12,13] Calculated velocity magnitudes and cross-section vector plots are shown in Figs. 9 and 10. Although experimental comparisons have not yet been made, the results are qualitatively correct. An effort is being made to obtain a turbulent flow solution at a much higher Reynolds number.

Conclusions

The code in its present form is still a research code. Considerable work remains to make the code operational in geometry of practical interest and at appropriate Reynolds number and with the turbulence model activated. Detailed documentation of the finite difference equations used exists in the form of informal notes only.

The leading-edge problem (i.e., going from a periodic upstream flow region into the blade region) has not been addressed.

The upstream flowfield must be specified very carefully. The flow angles must match the surface angles very accurately. The upstream cross-flow velocity distribution implies a streamwise velocity gradient distribution (because of the local continuity equation). Therefore, if the upstream cross-stream pressure gradients are not consistent with cross-stream velocities, drastic and unrealistic corrections will result at the first marching station, making it impossible to satisfy local continuity.

Moore and Moore[4] have described a method for calculating three-dimensional viscous flow through a rotating centrifugal impeller. Moore's method is partially parabolic; several complete streamwise marching passes through the impeller passage are required. Calculations have been made with a rather sparse mesh (13×13 on the cross section). The Moore code is proprietary and is not available to the public.

References

[1]Patankar, S. V. and Spalding, D. B., "A Calculation Procedure for Heat, Mass and Momentum Transfer in Three-Dimensional Parabolic Flows," *International Journal of Heat and Mass Transfer*, Vol. 15, Oct. 1972, pp. 1787-1806.

[2]Briley, W. R. and McDonald, H., "Three-Dimensional Viscous Flows with Large Secondary Velocity," *Journal of Fluid Mechanics*, Vol. 144, July 1984, pp. 47-77.

[3]Davis, R. T. and Rubin, S. G., "Non-Navier Stokes Viscous Flow Computations," *Computers and Fluids*, Vol. 8, No. 1, March 1980, pp. 101-131.

[4]Moore, J. and Moore, J. G., "Calculations of Three-Dimensional, Viscous Flow and Wake Development in a Centrifugal Impeller," *Performance Prediction of Centrifugal Pumps and Impellers*, ASME, New York, 1980.

[5]Katsanis, T., "Application of the Contravariant Form of the Navier-Stokes Equations," NASA TM-83448, 1983.

[6]Walkden, F., "The Equations of Motion of a Viscous, Compressible Gas Referred to an Arbitrarily Moving Co-ordinate System," Royal Aircraft Establishment, TR 66140, 1966.

[7]Baldwin, B. S. and Lomax, H., "Thin Layer Approximation and Algebraic Model for Separated Flows," AIAA Paper 78-257, Jan. 1978.

[8]Hughes, W. F. and Gaylord, E. W., *Basic Equations of Engineering Science*, McGraw-Hill Book Co., New York, 1964.

[9]Steger, J. L., "Implicit Finite-Difference Simulation of Flow about Arbitrary Two-Dimensional Geometries," *AIAA Journal*, Vol. 16, July 1978, pp. 679-686.

[10]Pulliam, T. H. and Steger, J. L., "Implicit Finite-Difference Simulations of Three-Dimensional Compressible Flow," *AIAA Journal*, Vol. 18, Feb. 1980, pp. 159-167.

[11]Viviand, H., "Conservative Forms of Gas Dynamic Equations," *La Recherche Aerospatiale*, No. 158, Jan.-Feb. 1974, pp. 65-66.

[12]Katsanis, T. and McNally, W. D., "Revised FORTRAN Program for Calculating Velocities and Streamlines on the Hub-Shroud Mid-channel Stream Surface of an Axial-, Radial-, or Mixed-Flow Turbomachine or Annular Duct. I-Users Manual," NASA TN-D-8430, 1977.

[13]Katsanis, T., "FORTRAN Program for Calculating Transonic Velocities on a Blade-to-Blade Stream Surface of a Turbomachine," NASA TN-D-5427, 1969.

[14]Denton, J. D., "An Improved Time Marching Method for Turbomachinery Flow Calculation," ASME Paper 82-GT-239, April 1982.

[15]Varga, R. S., *Matrix Iterative Analysis*, Prentice-Hall, Englewood Cliffs, NJ, 1962.

[16]Taylor, A. M. K. P., Whitelaw, J. H., and Yianneskis, M., "Curved Ducts with Strong Secondary Motion; Velocity Measurements of Developing Laminar and Turbulent Flows," *Journal of Fluids Engineering*, Vol. 104, No. 3, Sept. 1982, pp. 350-358.

[17]Reyhner, T. A. and Flugge-Lotz, I., "The Interaction of a Shock Wave with a Laminar Boundary Layer," *International Journal of Non-Linear Mechanics*, Vol. 3, 1968, pp. 173-199.